Vacuum 142 (2017) 114–122

Contents lists available at ScienceDirect

Vacuum

journal homepage: www.elsevier.com/locate/vacuum

Energy absorption during pulsed electron beam spot melting of 304 stainless steel: Monte-Carlo simulations and in-situ temperature measurements

P.R. Carriere*, Stephen Yue

Department of Mining and Materials Engineering, McGill University, Montreal, QC, H3A 2B2, Canada

ARTICLE INFO

Article history:
Received 24 April 2017
Accepted 29 April 2017
Available online 8 May 2017

Keywords:
Electron beam melting
Stainless steel
Energy absorption
Heat transfer
In-situ thermocouples
CASINO

ABSTRACT

The absorption coefficient during pulsed, conduction-mode electron beam spot melting of 304 stainless steel was measured at different combinations of accelerating voltage [60,80] kV, beam current [10,15,20] mA, pulse length [0.6–12] mS and beam inclination angle [0, 15, 35, 55, 65]°. Ignoring evaporative and radiative heat loss, the absorption coefficient was determined directly by fitting in-situ thermocouple measurements to an analytical function, with an average adjusted R-square fit parameter of 0.9996 over the 103 measurements. The absorption coefficient was found to be insensitive to both beam current and accelerating voltage, but decreased with increasing inclination angle. Measurements are compared to estimates generated from Monte-Carlo electron trajectory simulations using the CASINO software, with good agreement for all process parameter combinations, experimentally demonstrating the capability of Monte-Carlo methods to estimate local electron beam heat transfer.
© 2017 Elsevier Ltd. All rights reserved.

1. Introduction

Electron beam heat transfer models are based on accurate initial data regarding the material properties and absorbed beam energy. While the temperature-dependent material parameters can be determined using ex-situ techniques, the absorbed energy is often process dependent, and scaled according to the incident energy via the prefactor η, commonly referred to as the absorption coefficient or beam efficiency.

In one example, welding process models are calibrated against a variety of experimental results; including transient temperature measurements and metallurgical examination of the weld zone. Since the absorbed energy impacts both quantities, the η parameter is adjusted until sufficient agreement between experiment and model is obtained [1,2].

Thermocouples (TC) are a commonly used temperature sensor, as they are reliable, inexpensive and simple. Yet with shrinking the process domains and interaction times, careful consideration regarding the sampling frequency, junction size, positioning, joining method and response time are required [3]. These issues can pose challenges when measuring transient processes such as electron beam welding, drilling and powder bed fusion.

One solution is a calorimetric approach, whereby the material is heated in a thermally isolated fixture and the absorbed energy is determined by comparing the temperature rise to the net enthalpy increase. The technique was used to determine η during CO_2 laser irradiation, and supported process-microstructure modelling of eutectic Al-Cu 33 wt% and single-crystal nickel superalloy [4–6]. It has also been used to estimate the energy absorption of Inconel 706 during keyhole-mode electron beam welding [7].

More recently, in-situ TCs have been used to calibrate heat transfer models of electron beam powder bed fusion (EB-PBF) of 316L stainless steel and laser powder bed fusion (L-PBF) of Inconel 718 [8–10]. Thermocouples have also supported Directed Energy Deposition (DED) modelling and calibrated the effective emissivity of solid and powder material at high temperatures [11–14].

In some cases, in-situ measurements are supplanted by computational fluid dynamics models, which include the effects of buoyancy and Marangoni convection, latent heat, evaporation and mushy-zone heat transfer. The complexity of these models is sufficient to directly capture the volumetric heat transfer and the resulting weld zone characteristics. Good model agreement was achieved for explosive backing keyhole-type electron beam drilling of steel using an absorption coefficient of $\eta = 0.99$ and a beam peak power density (PPD) $\approx$ 10 kW/mm^2 [15]. A value of $\eta = 0.2$ was

* Corresponding author.
E-mail address: paul.carriere@mail.mcgill.ca (P.R. Carriere).

http://dx.doi.org/10.1016/j.vacuum.2017.04.039
0042-207X/© 2017 Elsevier Ltd. All rights reserved.

used to model keyhole-mode electron beam welding of 304 stainless steel over a range of PPDs (8–34 kW/mm^2), although the details regarding keyhole reflections are unclear [16]. A model for Nd:YAG laser spot welding of 304 stainless steel using $\eta = 0.27$ at PPDs of 2–6 kW/mm^2 accurately captured many of the process details, including fusion zone shape and alloy evaporation [17].

This manuscript details a new technique for measuring the conduction-mode absorption coefficient, η, for millisecond electron beam interactions at PPDs less than 2 kW/mm^2. Using a combination of precisely timed electron beam pulses, a novel process geometry, fast response thermocouples, and non-linear curve fitting, η is uniquely determined over 103 pulsed spot melting experiments. Agreement between experiment and Monte Carlo simulations is shown over a range of beam parameters, including variations in accelerating voltage, beam current, pulse length and incidence angle [18].

Monte Carlo simulations were conducted using the open-source software CASINO in order to generate the Back-Scattered Electrons (BSE) energy spectrum, which is then summed to give the energy reflected out of the sample. Previously, this software was used to examine the heat penetration depth during poly-energetic electron beam ablation, as well as the depth-dose effects during Critical Energy Electron Beam Lithography of insulating substrates [19–21]. CASINO has also been used to estimate the beam diameter growth during EB-PBF of 316L stainless steel [22]. Klassen et al. calculated the absorbed electron beam energy using semi-empirical equations, but measurements at power densities sufficient for melting were not provided [23]. As far as the authors are aware, this work represents the first experimental validation high power electron beam energy absorption using Monte-Carlo techniques.

2. Methods and materials

2.1. Electron beam energy balance

Each individual absorption measurement is defined by a spot melt of incident pulse energy:

$$Q_p = V_o I_b \tau \tag{1}$$

where Q_p, V_o, I_b and τ are the pulse energy, accelerating voltage, beam current and pulse length, respectively. During electron beam heating, the incident beam energy is divided among four dominant heat transfer mechanisms:

$$Q_p = Q_{BSE} + Q_{evap} + Q_{rad} + Q_c \tag{2}$$

where Q_{BSE}, Q_{evap} and Q_{rad} are the energy loss terms associated with Back-Scattered Electrons (BSE), evaporative cooling and radiative cooling, respectively. The remaining conduction heat, Q_c, is transported through the solid according to Fourier's law. A schematic diagram of these heat transfer mechanisms is shown in Fig. 1.

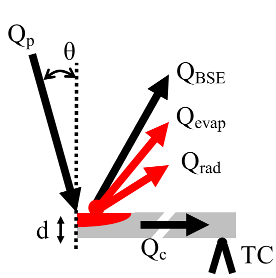

Fig. 1. Schematic of dominant electron beam energy balance terms, applied to an axis-symmetric geometry.

Terms associated with X-ray generation, secondary electrons (SE), beam transit losses and convective cooling have been omitted, as they form a negligible fraction of the energy balance during high-vacuum electron beam melting experiments [24]. Also, the heat carried by melt expulsion and vapor shielding will be ignored.

To facilitate process comparisons, Eq. (2) is normalized with respect to Q_p, yielding:

$$1 = \Gamma_{BSE} + \Gamma_{evap} + \Gamma_{rad} + \eta \tag{3}$$

where Γ_i is the respective fraction of energy transported out of the sample, while the absorption coefficient, η, represents the fraction of incident energy transported through the solid, Q_c/Q_p.

Whereas, the evaporative and radiative terms are only activated at high temperatures, the Γ_{BSE} term in Eq. (3) is intrinsic to the electron beam physics, a feature highlighted by the color coding of Fig. 1.

To facilitate comparison to simulations, it will prove useful to define η_0 according to:

$$\eta_0 = 1 - \Gamma_{BSE} \tag{4}$$

which represents the fraction of available incident beam energy, under the condition that $\eta_0 \leq 1$. Eq. (4) enables comparisons to laser-based processes, recognizing that the laser equivalent of Γ_{BSE} is the surface reflectivity, R. Substituting Eq. (4) into the normalized energy balance of Eq. (3) gives:

$$\eta_0 = \Gamma_{evap} + \Gamma_{rad} + \eta \tag{5}$$

It is worth discussing a few characteristic examples that demonstrate the dependencies of Eq. (5). In the simplest example, during scanning electron microscopy, the beam power is so low that the local temperature rise at the irradiation point is negligible, implying that $\Gamma_{BSE}, \Gamma_{evap} \rightarrow 0$ and $\eta_0 = \eta$. Conversely, in order to suppress the formation of a heat affected zone, femto-second laser machining requires that $\Gamma_{evap} \rightarrow \eta_0$, resulting in $\eta \rightarrow 0$ [25]. During laser surface remelting of Al-Cu33, it was found that η_0 was dependent on the material state (liquid/solid), implying that η_0 and η are coupled via the local enthalpy rise [4]. As a final example, the formation of a vapor capillary during keyhole welding requires $\Gamma_{evap} > 0$. Although counter-intuitive, this actually increases η_0, since the vapor capillary focuses the reflected energy back into the sample [24].

These examples highlight the subtle distinctions between the far-field temperature response associated with the η term and the local energy absorption, associated with the η_0 term. In other words, an η_0 fraction of incident energy can be converted to evaporative or radiative energy, whereas an η fraction of incident energy is conducted far from the spot melt, after these extrinsic heat transfer mechanisms have been removed from the energy balance.

This manuscript outlines experiments whereby the electron beam is pulsed onto a thin sheet of 304 stainless steel (SS304), resulting in a localized, conduction-mode spot melt. A thermocouple joined to the backside of the sheet records the temperature response of the pulse, as per the schematic of Fig. 1. The physio-spatial dimensions of the pulse, sheet and thermocouple (TC) are chosen so that the temperature response can be analytically described by an instantaneous line source of energy $Q_c = \eta Q_p$. Thus, the absorption coefficient associated with far-field heat conduction is directly extracted as a fit parameter from the TC measurements over a wide range of process configurations. Open-source Monte Carlo methods are used to estimate η_0 and these values are compared to experiment.

Download English Version:

https://daneshyari.com/en/article/5468062

Download Persian Version:

https://daneshyari.com/article/5468062

Daneshyari.com